



## The effects of multiple detonation waves in the RDE flow field

*Bayindir H. Saracoglu*

*Department of Aeronautics and Aerospace, von Karman Institute for Fluid Dynamics*

*Senior Research Engineer*

*1640 Sint-Genesius-Rode, Belgium*

*bayindir@saracoglu.co.uk*

*Aysu Ozden*

*Department of Aeronautics and Aerospace, von Karman Institute for Fluid Dynamics*

*Graduate Student*

*1640 Sint-Genesius-Rode, Belgium*

### ABSTRACT

Rotating detonation engines (RDE) promise a highly efficient future combustion process due to elevated temperature and pressure attained at high frequencies. Variety of the studies in the literature are devoted to understand the physics of detonation in RDE with combustion across single wave. The current study investigates the effects of multiple detonation waves through numerical simulations performed with an open source unsteady Reynolds-averaged Navier-Stokes solver, OpenFoam. The solver used was able to capture deflagration-to-detonation transition of the hydrogen-air mixture with a devoted tool called ddtFoam. To observe the effects of multiple detonation waves, a flow field with two shocks was implemented. Different inlet total pressures were applied to observe the effect of the inlet pressure on downstream flow field. Comparison in terms of Mach number, outlet flow angle, thrust force, total pressure and temperature had done for one shock and two shocks cases at baseline conditions.

**KEYWORDS** : *rotating detonation engines, multiple shockwaves, OpenFoam, combustion*

### NOMENCLATURE

PDE – Pulsed Detonation Engine

RDE – Rotating Detonation Engine

URANS – Unsteady Reynolds-Averaged Navier-Stokes

D – diffusion speed, m<sup>2</sup>/s

F – thrust, N

T – temperature, K

U – velocity, m/s

c – reaction progress variable

p – pressure, Pa

r – radius, m

t – time, s

dr – edge length of a computational cell in radial direction, m

dθ – edge length of a computational cell in angular direction, rad

dt – infinitesimal time step, s

α – flow angle, degrees

ρ – density, kg/m<sup>3</sup>

τ – autoignition delay time

v – velocity, m/s

ω – source term, kg/(m<sup>3</sup>s)

ignition – ignition time

i – inlet

o – outlet

y – circumferential direction

z – axial direction





Voitsekhovskii presented the concept for rotating detonation engines in 1959 [7] however numerical studies had to be postponed due to lack of computational power to analyze the complex chemical reaction kinetics and gas dynamics [8]. The improvement in numerical methods and elevated computational power made the RDE simulation possible nowadays. Initial studies were conducted for two-dimensional models with Euler approach [3]. Then, three dimensional modeling took place with adaptive mesh refinement [9]. Schwer and Kailasanath did 2D Euler and 3D simulations with chemical reaction modeling [10,11]. For a combustor fed with H<sub>2</sub>-air mixture, Frolov et. al. [11] and Dubrovskii et. al. [12] worked on a 3D unsteady Reynolds-averaged Navier-Stokes (URANS) code with the assumption of one-step reaction scheme.

In this study open source URANS reactive flow solver is used to understand the flow physics with multiple detonation waves and different inlet pressures. RDE's with the existence of one and two detonation waves were simulated and the results were compared in terms of Mach number, total pressure and temperature. Also distance averaged total pressure and temperature profiles were obtained to have a better understanding. The results were further processed to obtain the unsteady flow angle and thrust for single and double shock configurations.

## 2 METHODOLOGY

### 2.1 Numerical Tool

An open source CFD solver OpenFoam was used to perform the numerical simulations for this study. The solver provides the flexibility to implement new modules developed in C++ for specific problems [14]. To simulate the physics of deflagration-to-detonation phenomena in a RDE, ddtFoam solver was used [15]. It is a density-based code which solves the unsteady, compressible Navier-Stokes equations equipped for high Mach number compressible flows shock capturing with HLLC scheme to determine all the convective heat fluxes [16-18]. Turbulence closure was attained through k- $\omega$  shear stress transport method [19]. Combustion is modeled with a reaction progress variable,  $c$  for each cell. When  $c=0$ , the particles inside the cell are taken as unburnt, when  $c=1$ , they are taken as burnt. O'Conaire's reaction scheme mechanism was used to model the combustion of hydrogen [20]. Arrhenius equations could be solved to model the detonation, but instead autoignition delay time was used since Arrhenius equations are stiff and require fine spatial discretization [16]. Autoignition occurs just after the local autoignition delay time passes. Autoignition delay time is a function of local temperature  $T$ , pressure  $p$ , and mixture composition. When pressure and temperature are high enough, autoignition delay time becomes smaller. A nondimensional variable  $\tau$  was introduced to describe the autoignition process:

$$\tau = \frac{t}{t_{\text{ignition}}} \quad (1)$$

When the ignition variable  $\tau$  reaches unity, it means ignition delay time has passed and mixture is considered as ignited. As long as  $\tau$  does not reach unity, the flow is assumed not to be ignited. Autoignition delay time is calculated with Cantera by using O'Conaire's reaction scheme mechanism and the results are stored in the solver. After introducing autoignition time delay, a transport equation governing the combustion process could be written as follows [19]:

$$\frac{\partial(\rho\tau)}{\partial t} + \nabla \rho\tau \cdot v = -\nabla \cdot \rho D \nabla \tau + \omega_{\tau} \quad (2)$$

$\omega_{\tau}$  appears as the detonation source term. Deflagration part of the deflagration-to-detonation process should also be taken into consideration. To model the deflagration combustion, Weller model was used [19].

## 2.1 Computational Domain and Boundary Conditions

The computational domain comprises a 300 mm long annular combustor chamber whose inner and outer diameters are 260 mm and 306 mm, respectively (Figure 3). The mesh is composed of uniformly spaced hexahedral cells with an edge of 2 mm. The final domain contains 865800 elements.

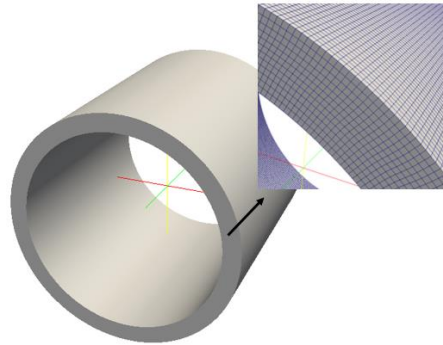


**Figure 3: RDE geometry and computational domain**

Inlet is modelled as an injector which feeds the combustion chamber continuously with stoichiometric  $H_2$ -air mixture at 293 K. On the wall boundaries, adiabatic, no-slip boundary condition is applied. To start ignition, a small zone at the inlet is initially charged with burnt mixture at high temperature and pressure. Number of detonation fronts is controlled by the initial conditions set at the inlet section of the RDE by setting high temperature and pressure zones where the detonation front is desired to be formed initially.

Data was probed from different locations on the flow domain. Since the major changes occur downstream of the detonation wave, locations chosen more frequently in this region. In total 22 probe locations were chosen in axial direction (Fig. 4-left). In the radial direction, data was probed for hub section at 15% of the domain thickness which is 133.45 mm, midspan section at 50% of the thickness which is 141.5 mm and shroud section at 85% of the thickness which is 149.55 mm. (Fig. 4-right). In total, there were 66 probe locations to monitor changes in the flow properties through the computational domain.

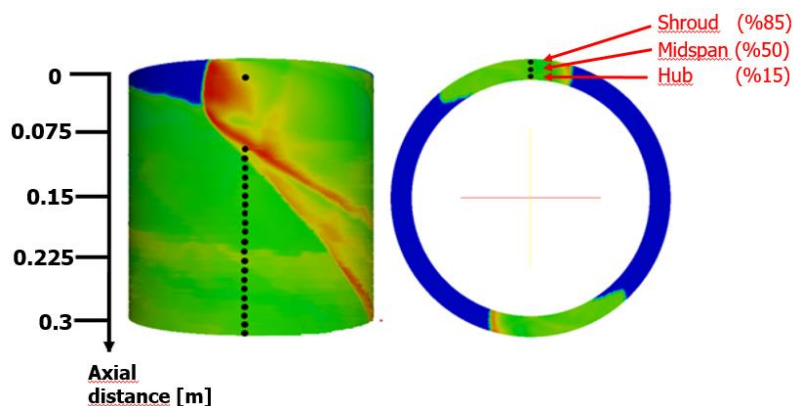


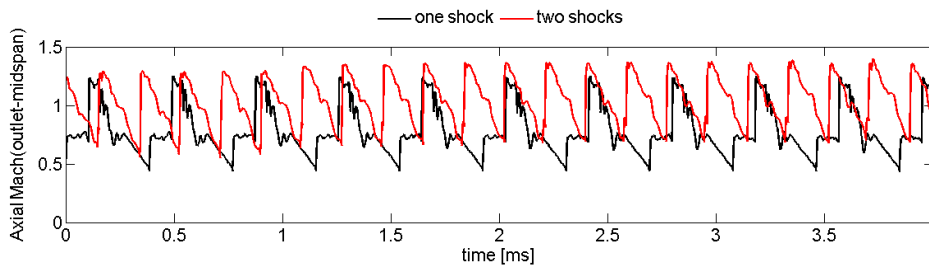
**Figure 4: Probe location in axial direction (left) and radial direction (right)**

## 3 RESULTS

The effects of multiple shock waves in a rotating detonation engine were investigated in comparison with the single detonation front. Inlet pressures of 4, 6, and 8 bar cases were analyzed to understand the result of inlet boundary conditions in terms of axial Mach number, flow angle, thrust force, total pressure and temperature of the flow.

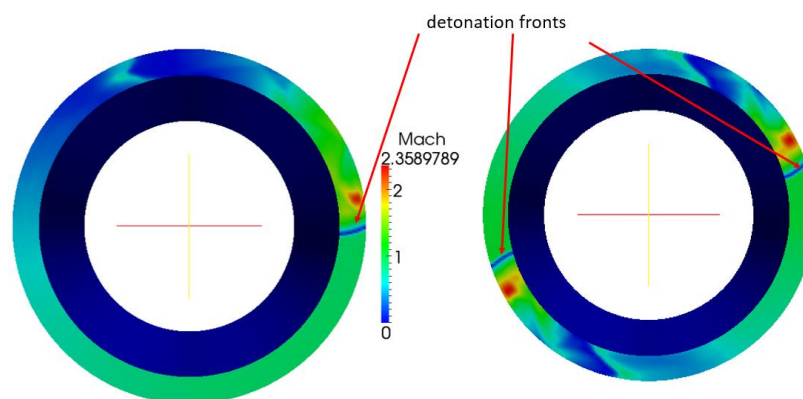
Firstly, the comparison between single shock and double shock cases were done at 8 bar inlet total pressure condition. The data from both simulations were extracted and plotted in the following figures to understand effects of the change in operation mode. In each figure, black and red lines represent one-shock and two-shock cases, respectively. All data was plotted between for 4 ms time interval after the URANS simulations were converged. For two-shock operation, 3 different inlet total pressures were investigated and the results were compared to understand the effects of the inlet conditions on the operation.

Figure 5 depicts the evolutions of the axial Mach number at the outlet. Mach number was calculated by using the flow velocity along the axial direction and the local speed of sound obtained from the properties of the mixture at each computational cell. Outlet Mach number stands for an important parameter to give an estimate on the variation of the thrust force which is one of the key performance parameters for an engine. Mach number evolution in time depicts that, for the same combustible mixture, two-shock operation provides a duty cycle frequency (5556 Hz) slightly above the double of one-shock (2631 kHz). Meanwhile, the peak axial Mach numbers at the outlet reaches the values around 1.3 which is higher than single-shock. Moreover, the minimum values stays higher than the single-shock operation all the time as the second shock prevents the flow to decelerate. Consequently, fluid force at the outlet is expected to be higher.



**Figure 5: Comparison of outlet Mach numbers for one shock and two shocks cases**

Zeldovich-Von Neumann-Doring (ZND) cycle accounts for a thin shock wave which is followed by a chemical reaction zone. It also states that the flow following the shock is subsonic, which indicates that the Mach number after the shock wave should be around 1. As can be seen in Figure 6, behind detonation front, there is a zone which has Mach number around 1, that shows both cases are in agreement with ZND detonation wave structure.



**Figure 6: One shock and two shocks cases Mach number contours, respectively**

Total pressure variations in time for one shock and two shocks cases is depicted in Figure 7. Blue line represents the total pressure level at the inlet of the combustor. The maximum outlet total pressure for single-shock can reach as high as 42 bars while the double-shock can generate total pressure peaks up to 23 bars. Hence, instantaneous pressure gain can reach 425% and 187% above the inlet

value for single and double shock cases, respectively. The time while the outlet total pressure is below the inlet total pressure reduces to less half of the single shock case.

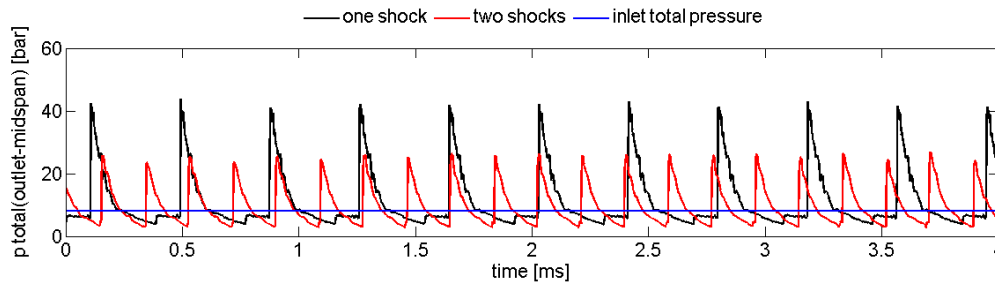


**Figure 7: Total pressure variations for one shock and two shocks cases**

Time-resolved analysis of the total temperature shows similar variations at the outlet for both operation mode. Nevertheless, **minimum** values do not go below 2000K for two-shock case while single-shock operation faces minimum temperature levels 200 K lower as compared to two-shock case. Moreover, high-frequency fluctuations in outlet temperature trace in single shock are also attenuated for two-shock case while the dominant frequency of the detonation front is doubled.

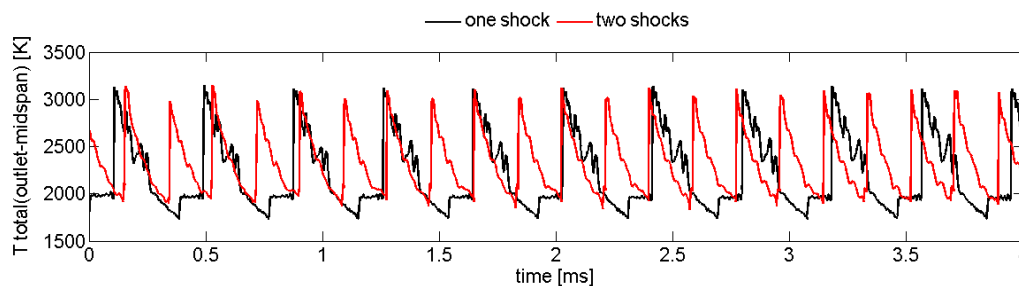


**Figure 8: Total temperature profile for one and two shocks cases at the outlet section**

In addition to the instantaneous variation of the flow properties, time-averaged evolution of the flow along the combustor was extracted at 3 span-wise locations on the annulus (15%, 50% and 85% of the channel height) on each of 20 axial locations. Eventually, time-averaged values at 3 span-wise locations are also averaged to achieve a single value for each axial stations. Figure 9 - top shows that the averaged pressure gain attained along the combustor is significantly higher for the one-shock as compared to two-shock operation. The gap stays around 1 bar all the way from 0.11 m until the outlet. The total pressure level, whereas, linearly reduces for both cases as the flow move towards the outlet. At the outlet, average pressure value for one shock case is around 1075 KPa and 975 KPa for two shocks. Consequently, the pressure gain with the RDE with respect to 8 bar inlet pressure results in 34% and 22% for one-shock and two-shock operation modes, respectively. On the other hand, the trend is inverted for the total temperature evolution along the engine (Figure 9-bottom). For two-shock case, the temperature level always remains above the one-shock and difference increases toward the outlet and reaches 100 K.

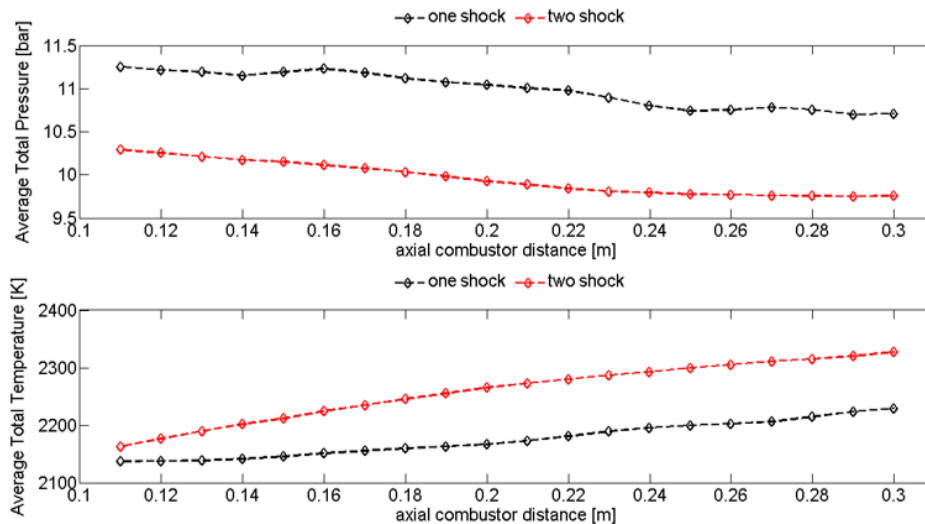


**Figure 9: Distance averaged total pressure and temperature values for one shock and two shocks cases**

Figure 10 depicts the effect of inlet conditions on the total pressure and total temperature variation along the combustor for two-shock operation mode. Three inlet total pressure were investigated at 4, 6 and 8 bars. The total pressure variation along engine shows a similar evolution for all inlet conditions. Eventually, at the outlet, the pressure difference between 4 bar to 6 bar cases yields to 2.8 and the difference between 6 bar to 8 bar cases yields to 1.95 bars. Although the pressure difference stands similar with each 2 bar increase on the inlet pressure, the overall pressure gain for each conditions differs. In other words, when the RDE is run with 4 bar, 6 bar and 8 bar inlet pressures, the total pressure gain at the outlet reaches to 25%, 30% and 22%.

When we look at the total temperature levels along the combustor, the intermediary inlet pressure results in the same increase in the temperature for the highest inlet pressure (Figure 10-bottom). Henceforth, within the given configuration driven by double shock wave, it can be concluded that the 6-bar inlet pressure is the optimum condition for the operation with the highest pressure gain and highest temperature rise. The lowest inlet pressure, on the other hand, results in 100 K lower outlet temperature than the other cases.

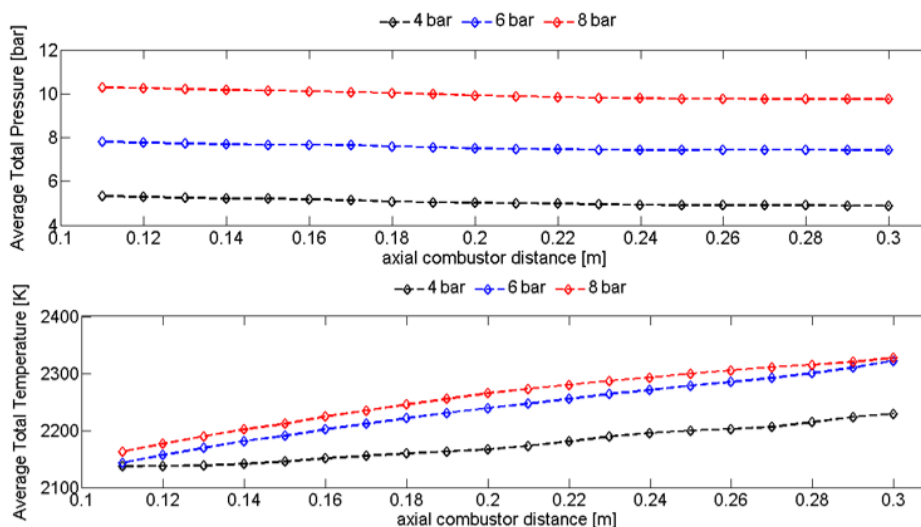


**Figure 10: Distance averaged total pressure and temperature values for all two shocks cases**

The outlet flow angle, defined as the angle form by the axial and circumferential components of the flow velocity (Eq. 3), remains the one of the important parameters for the propulsion purposes as the

axial component of the velocity provides the thrust for the aeroengines. In this regard, Figure 11-left compares the cases with one and two detonation waves. The angular variability in the outlet velocity is significantly reduced by the introduction of the second shock. The outlet flow angle varies between 20 to -50 degrees for single shock while it varies between 20 to -20 degrees for the double shock at the same inlet conditions. Consequently, the angular variation in flow is attenuated 43%.

$$\alpha = \tan^{-1} \left( \frac{U_y}{U_z} \right) \quad (3)$$

Lastly, the thrust that generated by the RDE for one-shock and two-shock operation was calculated in order to have a quantitative understanding of the propulsive characteristics of the engine (Eq. 4). Three inlet pressures were taken into consideration for two-shock calculations while a single inlet pressure was considered for one-shock case. The results shows that the thrust force linearly increases with the inlet total pressure fed to the RDE (Figure 11-right). The maximum value reached for two-shock case is 10 kN. However, it still stays 20% below the thrust provided with single detonation wave mode. Nevertheless, intermittency in the provided trust still remains an issue for one-sock case as the frequency of the detonation is 2631 Hz.

$$F = \left( \frac{1}{dt} \left( \iiint \left( (\rho U^2 r d\theta) dr \right) dt + \iiint \left( (p r d\theta) dr \right) dt \right) \right)_o - \left( \frac{1}{dt} \left( \iiint \left( (\rho U^2 r d\theta) dr \right) dt + \iiint \left( (p r d\theta) dr \right) dt \right) \right)_i \quad (4)$$

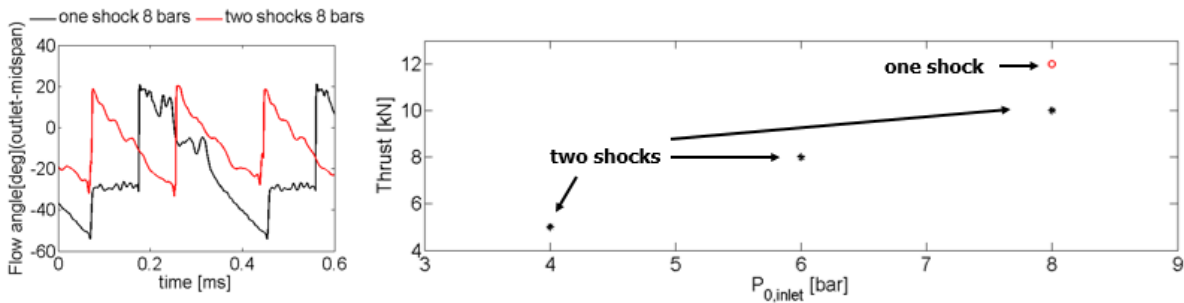


**Figure 11: Flow angle for one shock and two shocks cases (left), Time averaged thrust values for one shock 8 bar, and two shocks 4, 6, and 8 bar (right)**

#### 4 CONCLUSIONS

Detonation engines offer high thermal efficiencies owing to simultaneous pressure augmentation during heat addition by the constant volume combustion process. Rotation detonation engines stands as a promising alternative to modern heat engines working based on Bryton cycle thanks to high operational frequencies. The current study aims to investigate the effects of multiple shock waves on the operational characteristics of the RDE at different inlet pressures through reactive URANS simulations. Numerical simulation showed outlet flow field is significantly altered by the switch in the operational mode from one-shock to two shocks. The frequency of detonation is increased more than twice for double detonation wave configuration while the maximum outlet total temperature and axial Mach number levels are maintained at the same level. Whereas total pressure at the outlet was reduced almost double of the single-shock. Time-averaged results depicted that the two-shock configuration provides higher operational temperatures throughout the engine section following the detonation wave. However, the pressure gain is penalized by 12%. Consequently, the multiple detonation wave operation might be more suitable for power generation, especially from magnetohydrodynamic effect, while single detonation engine for propulsion application. The latter is also observed from the thrust calculation as the single shock wave provides higher thrust for the same inlet conditions. One should still keep in mind the bottleneck of low operational frequencies for one-shock mode though. Moreover, time-resolved outlet flow angle shows that the two-shock operation provides a lower variation on the outlet flow field. Therefore, multiple detonation waves can be a better candidate for engine configurations with downstream expander machinery such as turbines because lower variation in flow direction is one of the diminishing factor for unstart problem in



supersonic turbines. Finally, the effects of inlet conditions for multiple shock waves were investigated in terms of time-averaged pressure and temperature throughout the engine. The results showed that an optimum operation point can be achieved at 6 bars of inlet pressure as the total temperatures within the engine reaches a limit and doesn't significantly increase further even the inlet pressure is augmented.

## REFERENCES

1. E.M. Braun, F.K. Lu, D.R. Wilson, J.A. Camberos; 2013; "Airbreathing rotating detonation wave engine cycle analysis"; *Aerospace Science and Technology*; **27**; pp. 201-208
2. Y. Shao, M. Liu, J.P. Wang; 2010; "Continuous Detonation Engine and Effects of Different Types of Nozzle on Its Propulsion Performance"; *Chinese Journal of Aeronautics*; **23** (6); pp. 647-652
3. D.M. Davidenko, I. Gokalp, A.N. Kudryavtsev; 2008; "Numerical Study of the Continuous Detonation Wave Rocket Engine"; *15<sup>th</sup> AIAA International Space Planes and Hypersonic Systems and Technologies Conference*; Dayton, Ohio; 28 April-1 May
4. Y. Eude; 2011; "Développement d'un outil de simulation numérique des écoulements réactifs sur maillage auto-adaptif et son application à un moteur à détonation continue"; *PhD. Thesis*; Université d'Orléans; France
5. J. Braun, B.H. Saracoglu, T.E. Margin, G. Paniagua; 2016; "One-Dimensional Analysis of the Magnetohydrodynamic Effect in Rotating Detonation Combustors"; *AIAA Journal*; **54** (12); pp. 3761-3767
6. S.M. Frolov, V.S. Aksenov, V.S. Ivanov; 2015; "Experimental proof of Zel'dovich cycle efficiency gain over cycle with constant pressure combustion for hydrogen-oxygen fuel mixture"; *International Journal of Hydrogen Energy* 2015; **40**; pp. 6970-6975
7. B. V. Voitsekhovskiy; 1959; "A Stationary Detonation"; *Reports of USSR Academy of Sciences*; **29** (6); pp. 1254-1256
8. S. Zhdan, F. Bykovskii, E. Vedernikov; 2007; "Numerical Study of the Continuous Wave Rocket Engine"; *Combustion, Explosion and Shock Waves*; **43** (4); pp. 449-459
9. Y. Eude, D.M. Davidenko, I. Gokalp, F. Falempin; 2011; "Use of the Adaptive Mesh Refinement for 3D Simulations of a CDWRE (Continuous Detonation Wave Rocket Engine)"; *AIAA Paper*, 2011-2236
10. D. Schwer, K. Kailasanath; 2011; "Numerical Investigation of the Physics of Rotating-Detonation Engines"; *Proceedings of the Combustion Institute*; **33** (2); pp.2195-2202
11. D. Schwer, K. Kailasanath; 2011; "Numerical Study of the Effects of Engine Size on Rotating Detonation Engines"; *Proceedings of the 49<sup>th</sup> AIAA Aerospace Sciences Meeting*; AIAA Paper 2011-581
12. S. Frolov, A. Dubrovskii, V. Ivanov; 2013; "Three-Dimensional Numerical Simulation of Operation Process in Rotating Detonation Engine"; *Proceedings of the Progress in Propulsion Physics, EDP Sciences, France*; pp.467-488
13. A. Dubrovskii, V. Ivanov, S. Frolov; 2015; "Three-Dimensional Numerical Simulation of the Operation Process in Continuous Detonation Combustor with Separate Feeding of Hydrogen and Air"; *Russian Journal of Physical Chemistry B*; **9** (1); pp. 104-119
14. OpenFoam, "Official openfoam website" ; 2017; URL: <http://www.openfoam.com>
15. F. Ettner; 2017; "ddtFoam – OpenFOAM solver to simulate the deflagration-to-detonation transition"; URL: <http://sourceforge.net/projects/ddtfoam/>
16. F. Ettner, K.G. Vollmer, T. Sattelmayer; 2014; "Numerical Simulation of the Deflagration-to-Detonation Transition in Inhomogenous Mixtures"; *Journal of Combustion*; **2014**; pp.1-15
17. E.F. Toro, M. Spruce, W. Speares; 1994; "Restoration of the contact surface in the HLL-Riemann solver"; *Shock Waves*; **4** (1); pp.25-34
18. R.I. Issa; 1986; "Solution of the implicitly discretised fluid flow equations by operator-splitting"; *Journal of Computational Physics*; **62** (1); pp.40-65
19. J. Braun, B.H. Saracoglu, G. Paniagua; 2017; "Unsteady Performance of Rotating Detonation Engines with Different Exhaust Nozzles"; *Journal of Propulsion and Power*; **33**; pp. 121-130
20. M. Ó Conaire, H.J. Curran, J.M. Simmie, W.J. Pitz, C.K. Westbrook; 2004; "A Comprehensive Modeling Study of Hydrogen Oxidation"; *International Journal of Chemical Kinetics*; **36** (11); pp.603-622